Granular Matter (2023) 25:28
https://doi.org/10.1007/s10035-023-01318-x

ORIGINAL REPORT

On the dynamics of a liquid bridge between a sphere and a vertically vibrated solid surface

A. F. Vallone[1] · R. O. Uñac[1] · D. Maza[2] · A. M. Vidales[1]

Received: 5 September 2022 / Accepted: 16 February 2023

Abstract
This work presents an experimental study of the response of a liquid bridge formed between a sphere and a plane solid surface subjected to a vertical sinusoidal vibration. The amplitude and frequency of the oscillations can be varied. The successive movement of the particle along with the bridge deformation is registered to follow the dynamics of the system. The motivation is to figure out how capillary and viscosity forces can be modeled with the help of the experimental data obtained and to settle down a simplified theoretical approach capable of being implemented in the description of many phenomena involving wet granular grains. The results indicate that the viscosity effects can be neglected as soon as the amplitude of the movement is not too small, still obtaining a reasonable description of the dynamical behavior of the sphere/liquid-bridge system.

Keywords Capillary · Vibration · Viscosity · Liquid bridge

1 Introduction

The elementary scenario of a spherical particle deposited on a horizontal solid surface appears in a great number of physical and physicochemical problems. From the destabilization of grains on a sand pile to the adhesion of a micro particle to a rough substrate, that schematic image has served as the starting point for the design of many models for those diverse phenomena. Although apparently simple, the interaction between a particle and a wall surface possesses a great deal of complexity.

For the case of macroscopic grains (order of millimeters), the development of contact laws for particle-particle and particle-wall interactions has helped to improve the theoretical and numerical descriptions of the collective motion of granular matter [1], in such a way that successful models are presently used for predicting the behavior of grains in many different problems. Examples of these laws are the well-known Hooke and Hertzian elastic models applied to granular matter [2, 3], the Cundall and Strack model for particle friction [4], the spring-dashpot model [5] or the de Gennes model for "soft crust" particles [2], to name just a few of them. These laws are mostly based on the elastic behavior of dry solid bodies in touch, where linear or non-linear behavior can occur for the force-deformation response, depending on the particular materials involved.

Nevertheless, the presence of humidity in most real cases where particles and surfaces interact is unavoidable. Thus, the formation of capillary bridges is expected, adding a new component into the description of the forces involved.

The development of models including capillary effects has been successful in the last decades, helping to understand and predict the behavior of wet granular matter with good results [6–10]. In this way, both contact and capillary forces can be included in the theoretical modeling of particulate matter for a better approach to real scenarios. Just as an example, the complexity of the discharge of wet grains from a silo has been well predicted through Discrete Elements Methods several years ago [11].

In most cases, capillary forces can be considered as the result of a short range interaction [3] and are capable of forming strong networks when close packing of grains is present but, these networks can significantly decrease their strength as the spacing between particles increases, i.e., when capillary bridges are subjected to considerable

✉ A. M. Vidales
avidales@unsl.edu.ar

[1] INFAP, CONICET, Departamento de Física, Facultad de Ciencias Físico Matemáticas y Naturales, Universidad Nacional de San Luis, Ejército de los Andes 950, D5700HHW San Luis, Argentina

[2] Department of Physics and Applied Mathematics, University of Navarra, Pamplona, Spain

Published online: 09 March 2023

deformation, especially in two-particle configurations [12]. Consequently, there are still many features present when manipulating wet granular matter that still have to be studied in detail. For instance, the idea to model the interaction of a particle over a horizontal plane surface by using an elastic deformation of a virtual spring representing the contact can be adequate for dry matter but not when a liquid bridge is present at the interface between the two bodies or where adhesion plays an important role due to the size or the hardness of the particles involved [13, 14]. Needless to say when the volume of the liquid bridge is considerably higher and considerable stretching of it is expected. In that case, models have to be modified to account for the effect.

The study of the deformation of a liquid bridge under external excitations has been studied in the past motivated by the interest to grow crystals for semi-conductor applications and for the development of materials on board of space stations. Many researchers considered a mass of liquid (viscous or not) held by surface tension forces between two parallel, coaxial, solid disks and frequently under microgravity conditions, aiming at measuring the bridge frequency response and resonance frequencies [15].

Valsamis and coworkers also studied the excitation of a liquid bridge between two parallel plates (one fixed, one mobile) subjected to small vertical periodic perturbations and motivated by the possible applications in the problem of micro-assembly and control of micro-joints [16]. They used a Kelvin–Voigt model with spring, damper and inertial parameters, respectively. They found that this model was able to reproduce quite well most of the results for the micro liquid bridges used in their work.

The same configuration of a liquid trapped between two parallel surfaces but subjected to a horizontal vibration with small amplitude was studied by Ichikawa et al. [17]. By estimations of the intervening parameters, they were able to describe the experimental results using a fundamental mass-spring-damper approach with a reasonable agreement. On the other hand, the possible existence of a complex flow structure (like transversal vortices) inside a liquid bridge subjected to various horizontal vibrations was revealed in the numerical investigation by Liang et al. [18]. Similarly, small amplitude and low period vertical vibrations of a liquid bridge between two coaxial disks were presented in [19]. The author found analytically a criterion for the stability of the bridge, proving that the destabilizing role of gravity can be weakened or even eliminated by the effect of small vibrations. This finding was experimentally corroborated by Haynes and coworkers [20].

When the deformation of a liquid bridge is important and/or the velocity of that process is low, the viscous forces can be neglected [21–23]. Otherwise, viscosity has to be considered, increasing the complexity of the problem when variable velocities are present in the dynamics. A detailed study for the influence of viscosity forces in the strength of an oscillating pendular liquid bridge was studied by Ennis and co-worker three decades ago [24]. They assessed the relative contribution of static (capillary) and viscous forces for different capillary numbers (Ca) and concluded that, for Ca smaller than 10^{-3}, capillary effects prevails over liquid viscosity and relative particle motion but, for Ca greater than one, bridge strength is insensitive to surface tension and linearly related to Ca, resulting a function of viscosity at high Ca. Besides, discrepancies were found with theory when the bridge volume was small and the gap between the particles was large [22, 24].

Pitois et al. presented an extension of the classical formulations for capillary forces in order to include the dynamic effects in the strength of a capillary bridge between two particles [21]. They performed experiments and applied the extended formulation to describe the results. For a small volume of the bridge, the earlier expression due to Maugis was able to adequately describe the force in the problem [21, 25]. When viscous effects are present, a rate dependent term has to be introduced. The authors proposed a modified analytical expression directly related to the bridge volume and found accordance of the experimental results over a large range of liquid viscosity and particle velocity.

Sudo et al. [26] performed an experimental study of the behavior of a liquid bridge (water) between a solid sphere and a flat solid plate subject to vertical vibration. In particular, the volume of the bridge was less but close to the volume of the sphere. The authors found that the vibration acceleration dominated the behavior. At lower excitation accelerations (of the order of gravity) the sphere oscillated harmonically with a stable liquid bridge deformation. For higher acceleration excitation, the solid sphere exhibited a complicated response and the liquid bridge exhibited chaotic behavior [26].

A recent work by Buck et al., presented a numerical study of the collision of a particle with a wet horizontal plate [27]. They were able to predict the restitution coefficient for the particles when impacting normally and obliquely on the wet plate. The validation of the model was also a goal of the paper which presented the influence of collision parameters such as the velocity rate and angle of impact, the liquid properties and the possibility of rotation of the particle [27]. Although oscillations were not studied, the work by Buck demonstrated that the properties of the liquid layer wetting the plate have a strong influence on the normal restitution coefficient but it is nearly negligible for the tangential one and for rotation.

In the present study, we focus on the direct observation of the deformation of a liquid bridge formed between a sphere and a solid plane surface which is subjected to a sinusoidal vertical oscillation. The aim is at determining the dynamics of the bridge in such a complex scenario by following

the sphere's and the excited surface's movements. Different parameters are varied to assess the effects of the liquid volume and the frequency and amplitude of the excitation. Once the experimental data is recovered, a theoretical approach is developed in order to determine the role of the liquid bridge in the movement equation. An expression for the capillary force is proposed taking into account former models and evaluating the extent of the effects of the viscosity in the present scenario.

2 Experimental set-up and procedure

The experimental set-up shown in Fig. 1a is designed to study the liquid bridge dynamics. The device consists of a mechanical oscillator with an amplitude and frequency controlled externally by an electronic function generator.

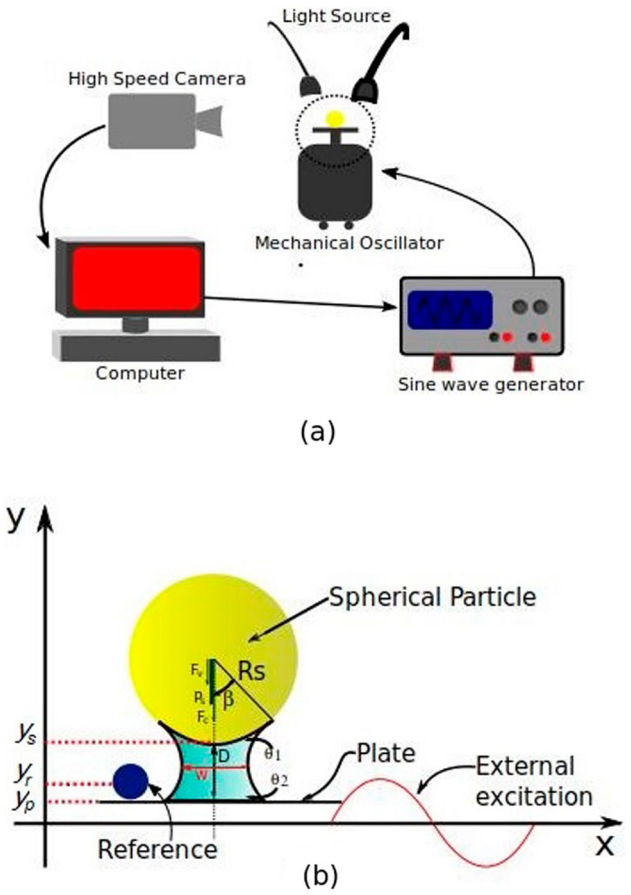

Fig. 1 **a** Sketch of the experimental set-up developed to measure the liquid bridge deformation indicating the different components. The circle indicates the amplified zone in part **b**. **b** Amplified sketch of the sphere indicating the main variables when the bridge is stretched. The bridge elongation is $D = y_s - y_p$, where y_p is determined through $y_p = y_r - R_r$ from the video processing. The contact angles θ_1 and θ_2 and the half filling angle β are indicated. The width of the bridge is W

A horizontal plane surface made in aluminum is fixed to the axis of the oscillator. On this surface, a known volume of liquid V (ethylene glycol) is placed and, immediately, a spherical and non-deformable particle (an air gun plastic bullet) with a diameter of 6 mm, a mass of 11 g and a volume greater than the liquid volume ($V_{bullet} = 0.11 \pm 0.03$ cm^3) is carefully placed on the middle of the liquid drop. The solid plane has a second smaller particle glued to it as a reference to follow the surface oscillation.

To follow the liquid bridge elongation two fast cameras are used depending on the needs: an IDS-UI3160CP for a preliminary study and a Photron Limited Mini UX100-Type 800 K-C-8GB for a systematic study. The maximum velocities employed during the recording are 1400 fps in the first case and 2000 fps in the second case. A PC captures all the video streaming for post processing with Matlab©.

The procedure to measure the behavior of the liquid bridge between the sphere and the surface when subjected to a sinusoidal excitation is the following. The desired liquid volume V of ethylene glycol is placed on the horizontal plate surface. This volume is controlled by first determining the weight of 10 ethylene glycol drops using a high precision balance. From an average over 10 separately equivalent determinations ($93 \pm 1 \times 10^{-3}$ g) and the ethylene glycol density $\rho = 1.11 \pm 0.01$ g/cm^3, the average volume for a drop results to be $84 \pm 2 \times 10^{-3}$ cm^3. Then, the spherical particle is deposited centered on the liquid volume. The desired frequency and amplitude A for the sinusoidal oscillation of the plate is chosen in the wave generator. The moving and reference spheres are filmed over a total of 20 oscillatory cycles. Once the recording is done, the oscillator is turned off. A new value for A and frequency are chosen and a new experiment is run by recording 20 cycles as before. The videos thus obtained are processed with Matlab©. The two different spheres are identified by the software through the entire movie and the stretching of the liquid bridge, D, is calculated from $D = y_s - y_p$, where y_s is the coordinate of the base of the big sphere (considered as a rigid body) respect to the fixed laboratory frame and y_p is determined through $y_p = y_r - R_r$, i.e., the difference between the mass center coordinate of the small reference sphere (respect to the fixed laboratory frame) and its radius, as they come from the imaging analysis. See Fig. 1b for definitions.

3 Experimental results

3.1 Preliminary tests

Before a systematic study, we perform several tests to find the optimal range of values to run the experiments avoiding the breaking of the liquid bridge and maximizing the acquisition speed. This speed depends on the size of each image,

the illumination and the oscillation frequency. After several tests, the following results are obtained.

3.1.1 Liquid volume

To select the parameter range for the experiments, it is interesting to evaluate the bridge final elongation, D_{max}, and final width, W_{max}, before its breaking as a function of the liquid volume V. Figure 2 shows the results for a fixed value of the amplitude at 3.35 mm. Figure 2a shows the values for D_{max} as a function of $V^{1/3}$. The positive correlation is evident from the figure, in agreement with the observations of former works [21, 28]. In the same way, when W_{max} is measured as a function of the volume of the liquid, the trend is also positive (Fig. 2b). The last point shows an important departure from the general trend. We attribute this difference to experimental problems in the image recording. On the other hand, the critical frequency for breaking increases linearly with the volume of the bridge, as shown in Fig. 2c. This is consistent with the expected increment of the capillary force as the volume of liquid increases [21, 28, 29].

3.1.2 Oscillation amplitude

In this part of our preliminary study, we observe the incidence of the amplitude of the sinusoidal oscillations, A, on the breaking of the liquid bridge. Experiments at different amplitudes (from 2.83 to 3.54 mm) are performed, and the results are shown in Fig. 3. The volume of the liquid bridge is fixed at 168×10^{-3} cm^3. It is important to point out that to find the critical frequency for breaking at a given A, we start the sinusoidal excitation of the plate from a very low frequency and increase this frequency at a given constant rate until the critical frequency value for breaking is reached. We observe that bridge rupture does not depend on the frequency rate of increment. Thus, to facilitate the processing time for the images, we chose for all the experimental runs a rate of 0.5 Hz/s, which is controlled automatically by the function generator.

Figure 3a shows the dependence between frequency and amplitude just before breaking. The curve indicates an exponential decay fitting to guide the eye. The behavior here resembles that found in [14] where a similar decaying trend was observed in the critical frequency-amplitude pairs for the detachment of dry particles at low humidity (less than 55%). Although a liquid bridge was not present in those experiments, the assumption of the presence of adhesion and low capillary effects as a linking bridge with elastic properties was assumed to model the experimental behavior with good results. In the present case, the linking bridge is the liquid one. The results found in this sub-section allow determining an adequate working range for the input frequencies to avoid the bridge breaking once the value for

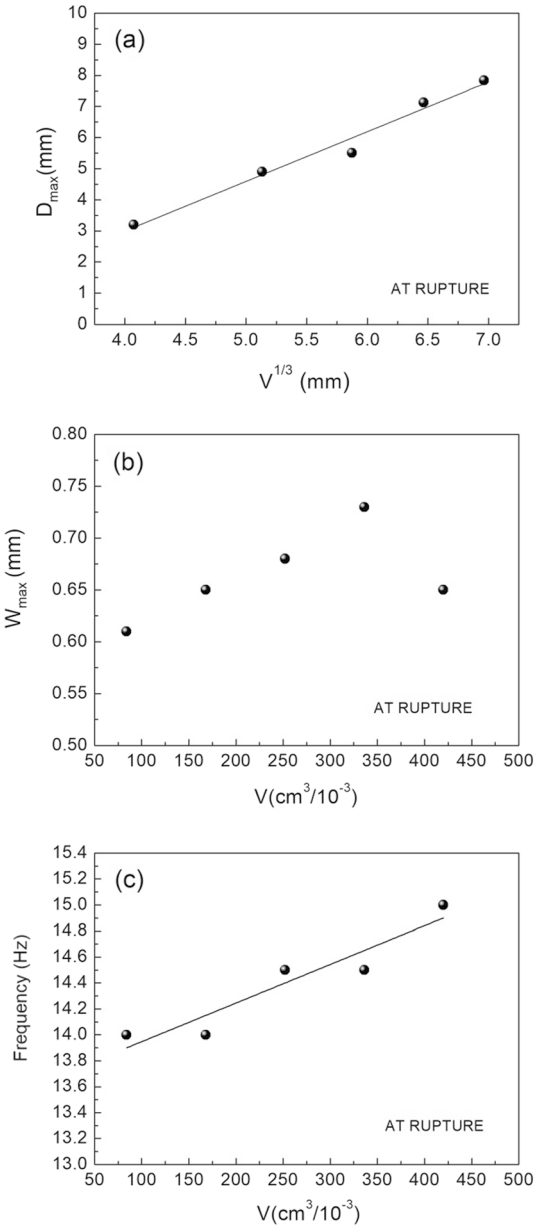

Fig. 2 Dependence of the dimensions of the liquid bridge on the liquid volume just before rupture happens for $A = 3.35$ mm. **a** Maximum elongation, D_{max}, before breaking. The line indicates a linear fit to highlight the $V^{1/3}$ correlation as in [21]. **b** Maximum width, W_{max}, before breaking. **c** Critical frequency just before rupture for the same system. The line is to guide the eye

A is chosen. The gray rectangle indicates the range for the systematic studied presented below.

On the other hand, the final elongation and width of the liquid bridge before breaking are shown in Fig. 3b. Both quantities practically do not depend on the amplitude of the excitations. This means that the elastic limit of the liquid bridge is surpassed after a certain critical ratio height/width is reached.

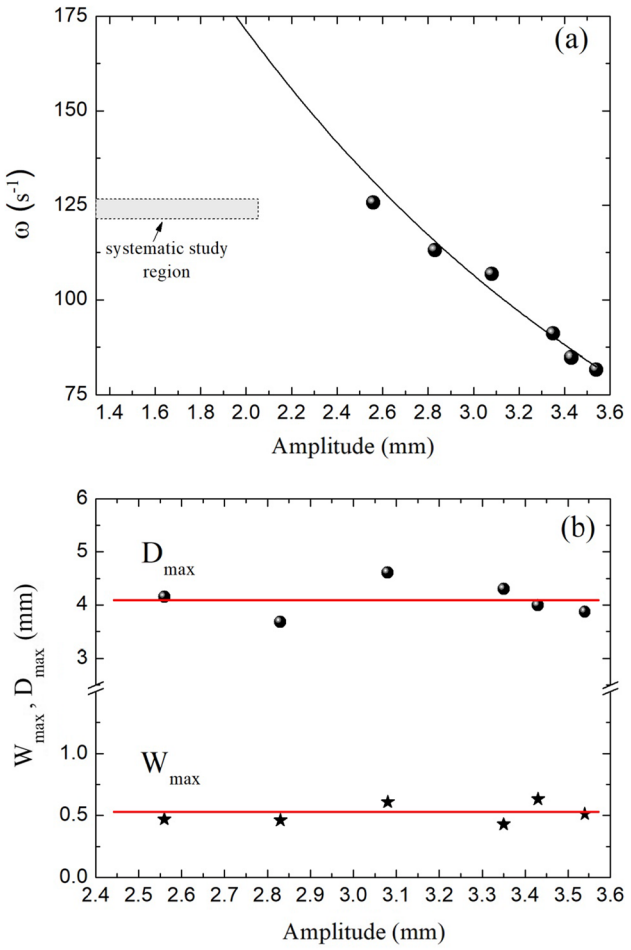

Fig. 3 **a** Critical angular frequency for bridge breaking as a function of the amplitude of the oscillations in the preliminary study. The curve is an exponential fit to guide the eye. The gray rectangle indicated the selected working zone for the systematic study at a fixed frequency of 20 Hz and variable amplitude. **b** Maximum height and width of the liquid bridge just before breaking and corresponding to the critical frequencies and amplitudes in part **a**

3.2 Systematic study

After the preliminary study shown so far, we present the results corresponding to the deformation of the liquid bridge between the sphere and the plane surface (plate) when a series of harmonic oscillations excite the plane. To avoid the breaking of the bridge but to have a measurable deformation, the working region selected is the one indicated in gray in Fig. 3a. In this study, all the experiments are performed at a fixed frequency of 20 Hz (125.66 s^{-1}) and a given fixed value of the amplitude. A total of 20 oscillatory cycles are recorded for a given A. Once the recording is done, the oscillator is turned off. A new value for A is chosen and a new experiment is run by recording 20 cycles as before. The values selected for A range from 1.34 to 2.03 mm.

Figure 4a shows an average over 20 cycles for $A = 1.45$ mm and a liquid volume of ethylene glycol equal to 23 mm^3. The time axis is set dimensionless by dividing the time by the oscillation period, T. The successive positions for the plate and the sphere are indicated. The elongation of the bridge is evident when the curve corresponding to the sphere (upper one) separates from the one of the plate, as the starry curve indicates. Were the upper curve the one corresponding to the excitation of a dry sphere on a plane, its shape would fit a parabola. Nevertheless, in this case, a different behavior is expected. The results for only one typical cycle of excitation are shown in the inset of the figure to evidence the confidence of the results comparing to the averaged ones.

The difference between the two curves (base of the sphere and plate position) represents the height of the capillary bridge or bridge elongation and it is plotted in Fig. 4b for different amplitudes, as indicated. Each plot corresponds to an independent run and is also an average over 20 cycles with the same value for A. The small shoulders at the right of the curves correspond to a slight rebound of the sphere once it touches the plate.

As the amplitude increases, thus the acceleration of the plate, the elongation of the bridge increases. The inset in the figure shows the correlation between A and the highest elongation attained by the bridge. It is important to remember that, in this case, the bridge dynamics is far from the breaking point. Two different regimes can roughly be distinguished in the inset. At lower amplitudes, the bridge is more resistant to deformation than for higher amplitudes, as evidenced by the change of slope in the plot. This is also observed for a different bridge volume. We think that one of the reasons for this apparent change of rigidity of the bridge is the fact that viscous effects are a little stronger for smaller amplitudes, as seen later in this work.

Figure 5 shows the average over 20 cycles for the trajectory followed by the sphere and the plate for the case $A = 1.95$ mm. Besides, the height of the liquid bridge and the numerical derivatives corresponding to the velocities for both trajectories are also plotted. Let us observe what is happening during the complete cycle of the movement. Different stages can be distinguished.

- From $t = 0$ to, approximately, $t = 0.2T$, the sphere is stuck to the plate. They have the same velocity and the bridge is not stretched.
- At $t = 0.2T$ the inertial force of the plate is enough to overcome the weight of the sphere and the capillary adhesion exerted by the liquid bridge.
- From $t = 0.2T$ to $t = 0.7T$, the sphere separates from the plate and the stretching period of the bridge takes place. Inside this stage, three different sub-stages can be discriminated. (1) First, the sphere detaches from

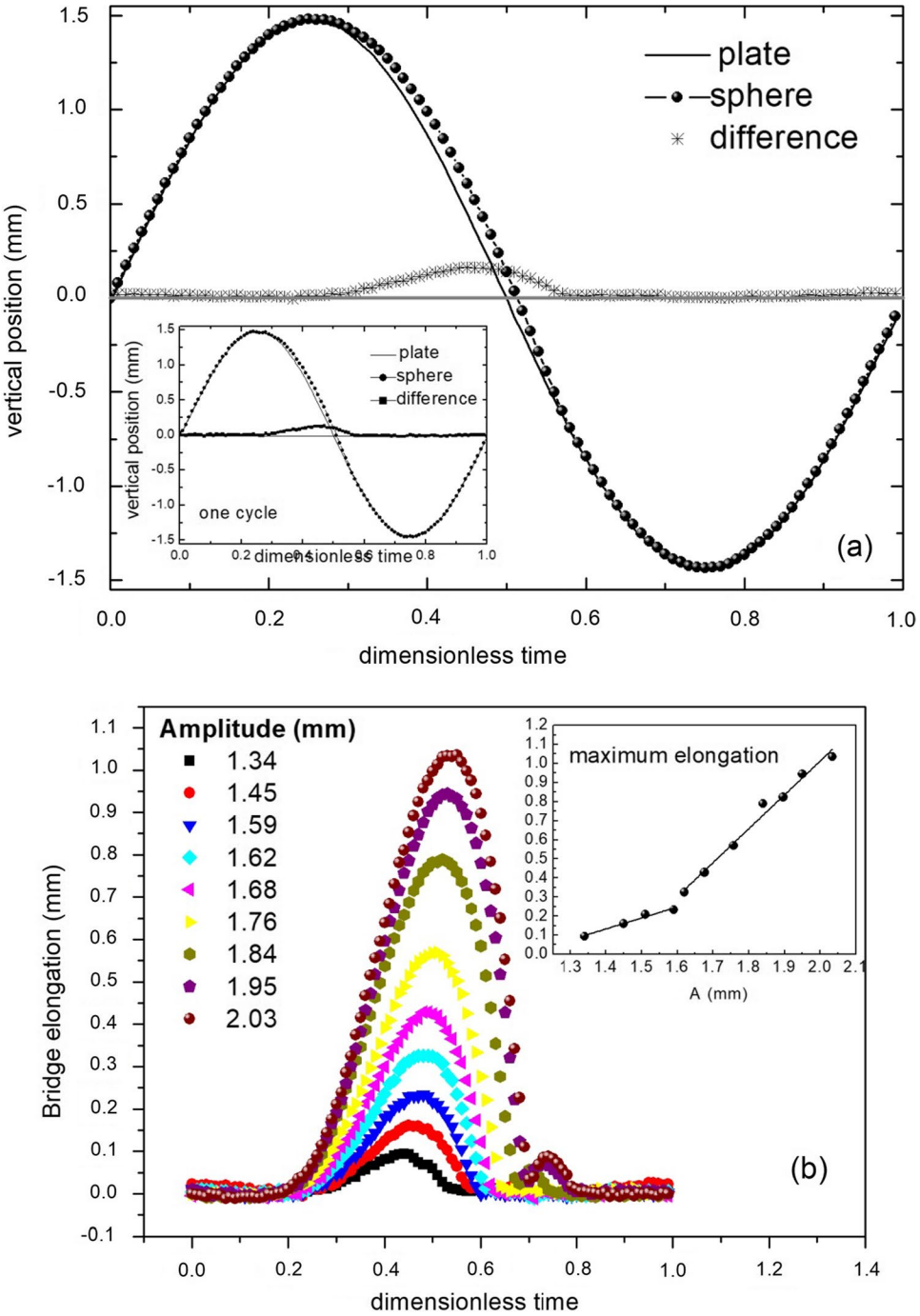

Fig. 4 **a** Average over 20 cycles for the bridge elongation (i.e. the difference between the position of the base of the sphere and that of the plate) versus dimensionless time (t/T) where T is the period of the oscillations. Here, $A = 1.45$ mm. The difference in positions is indicated. The inset shows the results for only one cycle to show the effect of the averaging on the results. Note that the movement is very well reproduced in each individual cycle. **b** Liquid bridge elongation versus dimensionless time taken as the difference between the curves like in **a**. The inset shows the correlation with A for the maximum elongation attained by the bridge

the surface with the same upward velocity of the plate. That velocity keeps greater than the upwards velocity of the plate because the deceleration of the plate is greater than that of the sphere. When the velocity of the plate is zero, it begins to increase downwards ($t \approx 0.25T$) while the sphere is still moving upwards and decelerated. (2) The second sub-stage begins when the sphere stops and starts to fall down with downward acceleration. Plate and sphere both go down with different velocities, the one of the plate being greater. After passing through its maximum value, the plate decelerates and the sphere's velocity equals that of the plate ($t \approx 0.52T$) and the stretching of the bridge becomes maximum. (3) The third sub-stage corresponds to the contraction of the liquid bridge. This is due to the inversion of the difference between the velocities, the one of the sphere being greater in this case. The contraction lasts until the sphere touches the plate and sticks again to it, rapidly matching the plate velocity and position ($t \approx 0.7T$).

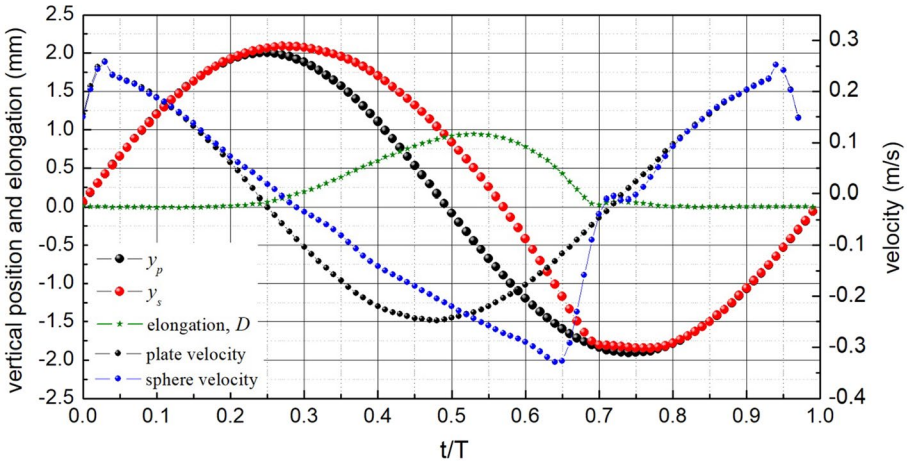

Fig. 5 Average oscillation cycle for $A = 1.95$ mm and 20 Hz. The position of the base of the sphere, y_s, and that of the plate, y_p, are plotted along with the bridge elongation $D(t)$ (left vertical axis) as a function of time. The numerical derivatives corresponding to the velocities of the sphere and the plate are also plotted (right axis)

- For $t > 0.7T$ the system sphere/plate behaves again in cohesion until a new cycle begins.

It is also interesting to note in Fig. 5 the way in which the velocity increases when the sphere is falling (from approximately $t = 0.26T$ to $t = 0.64T$). Although it could appear as linear, the acceleration is not constant. This would indicate a change in the capillary adhesion of the liquid bridge as it is stretched. We will come to this point below, when the theoretical model is proposed.

From the observations so far, it is clear that the response of the sphere to the oscillatory movement is not simple and that a simplified model representing the liquid bridge as a spring-damper system is not straightforward because of the complex relative movement between the particle and the plane. We need to investigate if a linearly decreasing force model for capillary interaction (like those proposed in [7, 21] or [29]) is still valid to describe the present scenario.

4 Dynamical behavior analysis

Figure 6 shows a series of snapshots for a typical stretching cycle of the liquid bridge. Given that the sphere is considered as a rigid body without deformation, we chose the vertical coordinate for locating the sphere the one corresponding to its base, $y_s(t)$. The one for the plane surface is $y_p(t) = A\sin(\omega t + \emptyset)$ with ω the oscillation angular frequency. Taking into account the forces acting on the particle, the following equation can be written:

$$m\frac{d^2y_s}{dt^2} = -F_c - F_v - mg \tag{1}$$

where m is the sphere's mass, g is gravity acceleration and F_c and F_v are the capillary and viscous forces, respectively.

To model the capillary force, we follow the expression given by Pitois et al. [21] and, more recently, also deduced by Butt and Kapple [29] and valid if the volume of the bridge is constant. In the present case, this assumption can be done because evaporation effects are negligible for ethylene glycol during the experiment duration [12]. In this way:

$$F_c = 4\pi\gamma BR_s\left(1 - \frac{D}{\sqrt{\frac{V}{\pi R_s} + D^2}}\right) \tag{2}$$

In Eq. (2), γ is the surface tension of the liquid interface, R_s is the sphere's radius, V is the bridge volume, $D = D(t) = y_s(t) - y_p(t)$ and $B = \frac{\cos(\theta_1+\beta)+\cos\theta_2}{2}$. The angles θ_1, θ_2, are the solid/liquid contact angles and β is the half filling angle (Fig. 1b). Although all the angles are expected to vary during the deformation of the liquid bridge, a detailed observation of the behavior of the contact angles θ_1 and θ_2 during our experiments reveals that they are practically constant during all the deformation process. For

Fig. 6 Sequence of photographs for the stretching of the liquid bridge

this reason, we cannot say that hysteresis is present up to the limit of our measurements precision. This is in coincidence with the observations by Buck et al. for the case of the rebounding of wet particles where the contact angle was practically constant for most of the bridge lifetime, except during the first millisecond [27]. Besides, the variation of B with time is bounded by the limiting values of both cosine functions. For that reason, it is expected from Eq. (2) that the strength of the capillary force decreases as the bridge is elongated.

The viscous force, F_v, is dependent on the rate of deformation $\frac{dD}{dt}$ [21]. As explained in the Introduction, if the deformation velocity is low, viscous effects can be neglected. In the present case, the highest velocity corresponds to the highest amplitude used in the experiments ($A = 2.03 \times 10^{-3}$ m) and, thus, the capillary number $C_a = \frac{A\omega\mu}{\gamma}$ results to be almost of the order of 10^{-1}, where μ is the dynamical viscosity of the fluid. For the same extreme case, the Reynolds number, $R_e = \frac{A\omega R_s \rho}{\mu}$, attains a maximum value equal to 53. It is known from the literature that a capillary number of the order 10^0 differentiates the response of a liquid bridge from being dominated by viscous forces ($C_a > 10^0$) of by capillary forces ($C_a < 10^0$) [21, 22, 24]. Here, the maximum values for C_a are close to one but they stay always less than the threshold value of 10^0. Thus, we cannot assure (unless we assess the forces) whether viscosity will play a role or not in our present scenario [21, 24]. The values attained by C_a all over the cycle of bridge stretching, for three different amplitudes, are shown in Fig. 7.

To model the viscous force we follow here the approach presented by Pitois et al. [21, 22] and compare the values of the forces thus computed with those for capillary effects. For the case of a finite volume for the liquid bridge, the expression for F_v becomes [21, 30]:

$$F_v = \frac{3}{2}\pi\mu R_s^2 \frac{1}{D}\frac{dD}{dt}\left(1 - \frac{D}{\sqrt{\frac{V}{\pi R_s} + D^2}}\right)^2 \tag{3}$$

In this way, Eq. (1) results the following differential equation:

$$m\frac{d^2 y_s(t)}{dt^2} = -4\pi\gamma B R_s\left(1 - \frac{D}{\sqrt{\frac{V}{\pi R_s} + D^2}}\right) - \frac{3}{2}\pi\mu R_s^2 \frac{1}{D}\frac{dD}{dt}\left(1 - \frac{D}{\sqrt{\frac{V}{\pi R_s} + D^2}}\right)^2 - mg \tag{4}$$

$$\text{with} \quad D = D(t) = y_s(t) - A\sin(\omega t + \emptyset)$$

As shown in Fig. 5, the values for $D(t)$ can be obtained from the experimental data. In order to elucidate whether the viscous effect can be neglected or not, we compute the capillary and viscous forces using Eqs. (2) and (3), respectively, and the experimental values for $D(t)$. In Fig. 8 the results are shown for six different values of the amplitudes employed. A normalized time is used by dividing the time coordinate by the total deformation time of the liquid bridge in each case. It is clear that the viscous force is most of the time smaller than the capillary one for all values of A. Nevertheless, for the smaller amplitudes, the relative effect of the viscous forces during bridge deformation is more important than for greater amplitudes.

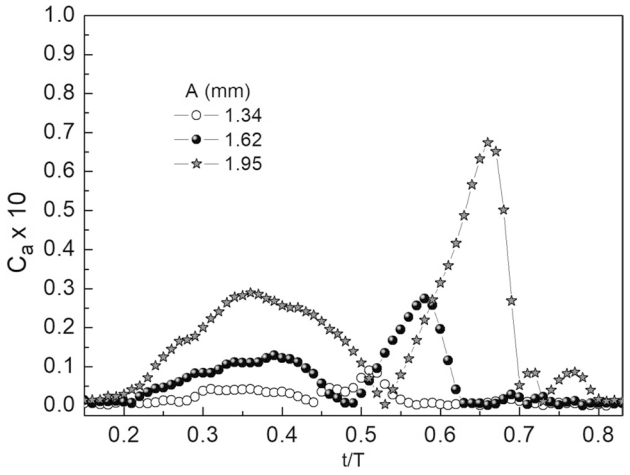

Fig. 7 Calculation of the Capillary Number, C_a as a function of dimensionless time during the deformation period of the liquid bridge. The values for the amplitude are indicated

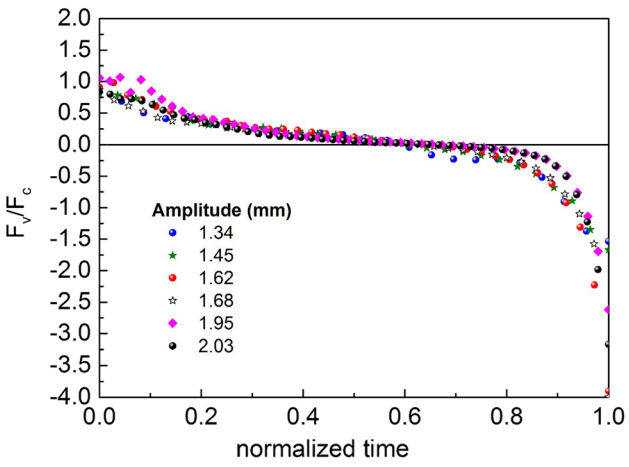

Fig. 8 Ratio F_v/F_c for three different values of A employed in the experiments as a function of the normalized time during one deformation cycle

In general, it is observed that for $A \geq 1.62 \times 10^{-3}$ m, viscosity effects are only important during the first milliseconds of the bridge stretching and the last milliseconds of the bridge contraction, otherwise, the incidence of F_v could be neglected. Consequently, and as a first approach, we will ignore in what follows the viscosity effects, analyzing the consequences of this theoretical assumption on the model prediction capability.

To make the solution of Eq. (4) more tractable, we evaluate the behavior of the term $\frac{D}{\sqrt{\frac{V}{\pi R_s}+D^2}}$ during a complete cycle of movement. Figure 9(a) shows the values of this term as a function of dimensionless time for the case of $A = 1.95$ mm. The solid line corresponds to a fitting curve with the form $\frac{D}{\alpha\sqrt{\frac{V}{\pi R_s}}}$, where $\alpha = 1.16$ and $V = 23$ mm^3. Coefficient α depends on the excitation amplitude, as illustrated in Fig. 9b. Figure 9c and d show the calculation of F_v with the fitting function. This approximation helps to simplify the resolution of the differential equation without losing the general trend of the reduction of the capillary force as the bridge is elongated.

Defining $F_0 = 4\pi\gamma BR_s$ and $L = \sqrt{\frac{V}{\pi R_s}}$, the simplified equation is now:

$$\frac{d^2y_s(t)}{dt^2} - \frac{F_0 y_s(t)}{\alpha mL} + \frac{F_0 A\sin(\omega t + \emptyset)}{\alpha mL} + \frac{F_0}{m} + g = 0 \tag{5}$$

In defining F_0, we take into account the fact that the value of B in time is bounded. Thus, F_0 holds in its value a time-average representative of the maximum capillary force involved in the whole dynamic process for a given value of A. Equation (5) can still be condensed further by defining $G_0 = \frac{F_0}{m} + g$ and $\omega_0^2 = \frac{F_0}{m\alpha L}$, giving:

$$\frac{d^2y_s(t)}{dt^2} - \omega_0^2 y_s(t) + \omega_0^2 A\sin(\omega t + \emptyset) + G_0 = 0 \tag{6}$$

The integration of Eq. (6) gives:

$$y_s(t) = \frac{A\omega_0^2\sin(\omega t + \emptyset)}{\omega^2 + \omega_0^2} + C_1 e^{\omega_0(t-t_0)} + C_2 e^{-\omega_0(t-t_0)} + \frac{G_0}{\omega_0^2} \tag{7}$$

For $t = t_0$, the height D of the bridge is zero. Thus, the acceleration of the plate and the sphere just before detaching (see Eq. (6)) is $a_0 = -A\omega^2\sin(\omega t_0 + \emptyset) = -G_0$. In the same way, the position of the base of the sphere is $y_s(t_0) = A\sin(\omega t_0 + \emptyset) = \frac{G_0}{\omega^2}$, and the velocity is

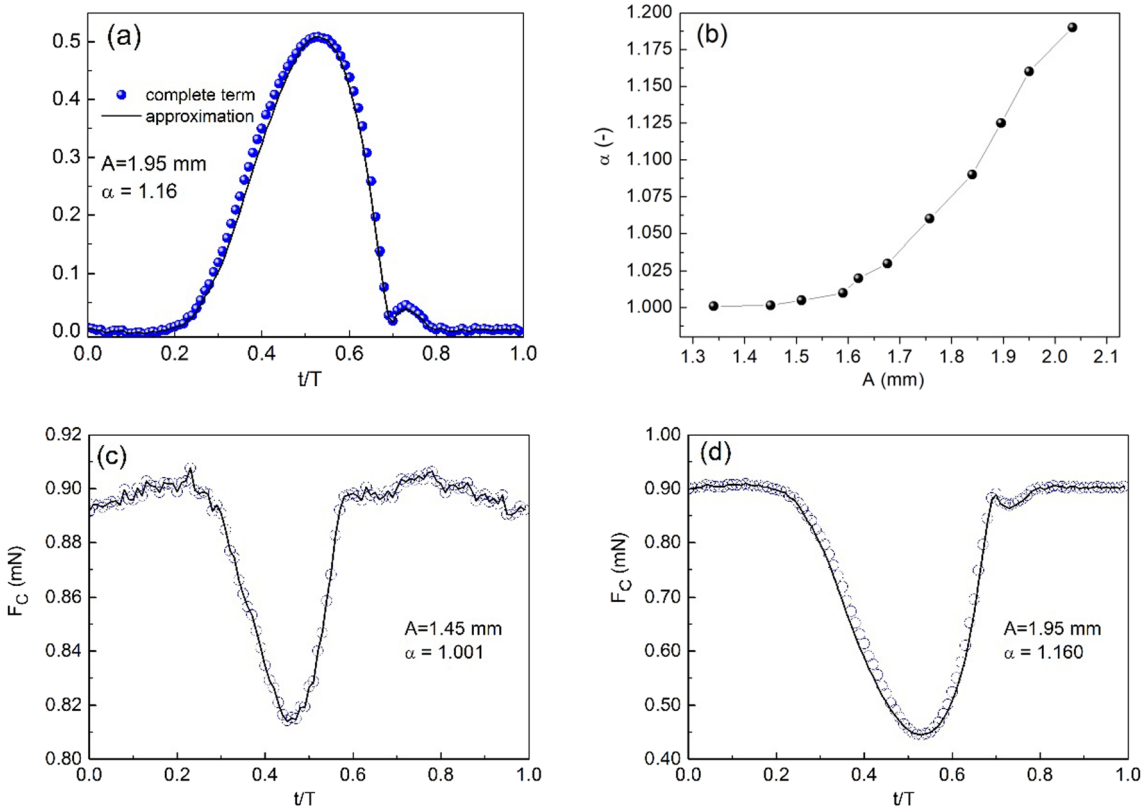

Fig. 9 **a** Representation of the term $\frac{D}{\sqrt{\frac{V}{\pi R_s}+D^2}}$ through the approximation $\frac{D}{\alpha\sqrt{\frac{V}{\pi R_s}}}$ for the case $A = 1.95$ mm. **b** Dependence of α on A. Examples of the approximation of F_c for two different amplitudes, **c** $A = 1.45$ mm and **d** $A = 1.95$ mm. The corresponding values of α are indicated

$v_0 = A\omega\cos(\omega t_0 + \emptyset) = \frac{\sqrt{A^2\omega^4 - G_0}}{\omega}$. Taking into account these initial conditions, the integration constants C_1 and C_2 result to be:

$$C_1 = \frac{\omega^2(v_0\omega_0 - G_0)}{2\omega_0^2(\omega^2 + \omega_0^2)}$$
$$C_2 = \frac{-\omega^2(v_0\omega_0 + G_0)}{2\omega_0^2(\omega^2 + \omega_0^2)} \quad (8)$$

5 Discussion

In implementing the above dynamical analysis, it is worthy to note the choice for a fitting of the experimental data with the function obtained from the integration of Eq. (7). It is important to remark that a single free fitting parameter is left once all the relations between the different variables are evaluated. This choice is based on the experimental difficulty in determining the exact moment at which the sphere detaches from the plate for the first time (t_0), in other words, to determine the initial conditions for the solution.

Figure 10 presents the comparison of the experimental data with the best fitting obtained using the solution in Eq. (7) for three different values of A. The theoretical description of the dynamics of the sphere is in agreement with the experiments, although the viscous term has been neglected in Eq. (5). Indeed, when comparing Fig. 10a with Fig. 10b and c, a better theoretical description is obtained as the value of the amplitude increases.

It is interesting to analyze the behavior of F_0 obtained from the different fittings as the amplitude of the oscillations is varied. Figure 11 shows the values. As the amplitude increases, the representative maximum force for the bridge stretching increases. This is explained by taking into account that F_0 is linearly related to $B = \frac{\cos(\theta_1+\beta)+\cos\theta_2}{2}$, i.e., to the geometry of the liquid bridge and its deformation over the cycle. As stated above, the contact angles are practically constant in time. On the other hand, when tracking the values of β along the experiments' videos, their variation is found to be more important as the amplitude increases. In other words, for low A, the value of beta is practically unaffected by the oscillations but, as A increases and the bridge elongates even more, the values of β markedly decrease and its average value does too. Figure 12 illustrates the behavior of β. The effect of an increasing F_0 with A should not be interpreted as an increment of the bridge strength. On the contrary, it is precisely the consequence of the weakening of the liquid bridge allowing a further deformation and, thus, a greater variation of the angle β.

The behavior of ω_0 against the amplitude is shown in Fig. 13. This quantity could be interpreted as a characteristic frequency for the sphere/liquid-bridge system, related to the mass of the sphere and the liquid properties and geometry. At low amplitudes, it is observed that ω_0 increases with A but reaches a plateau when

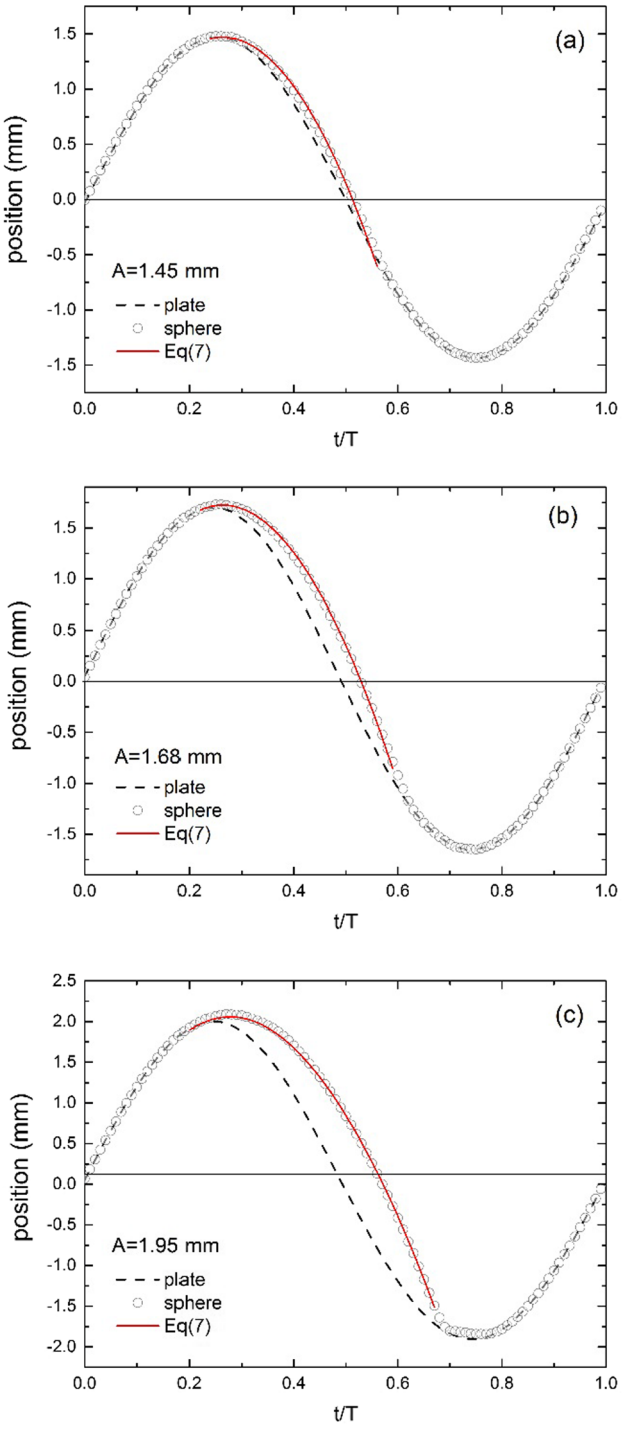

Fig. 10 Comparison between the theoretical prediction of Eq. (7) and the experimental data for **a** $A = 1.45$ mm; **b** $A = 1.68$ mm; **c** $A = 1.95$ mm. Note the enhancement of the fitting as the amplitude increases

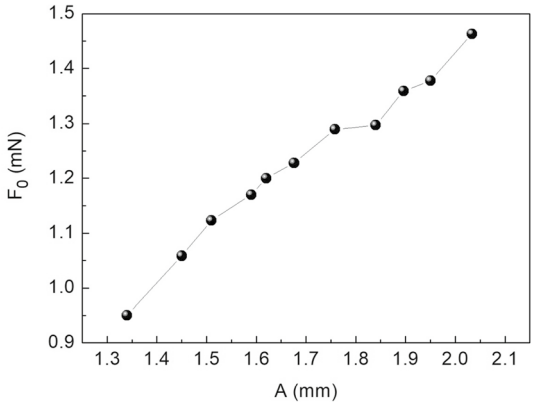

Fig. 11 Behavior of F_0as the amplitude of the oscillations increases

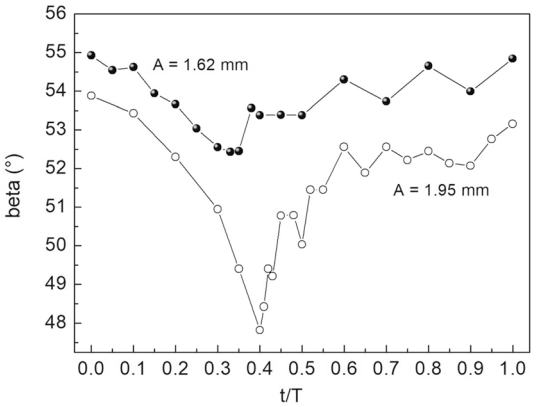

Fig. 12 Variation of angle β during a complete cycle of deformation of the liquid bridge, for two different amplitudes, as indicated. Note the different range of values taken in each case

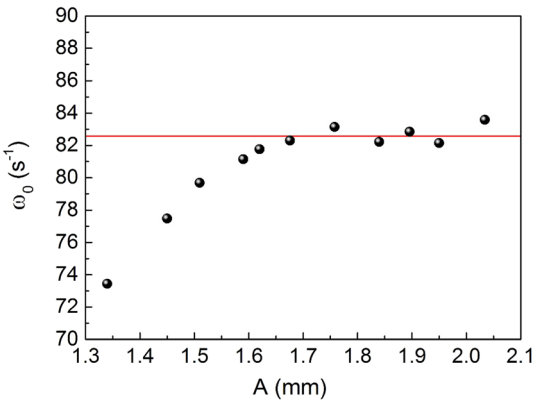

Fig. 13 Characteristic frequency of the sphere/liquid bridge system as a function of the amplitude of the oscillations. The line is an average over the last seven points to indicate the trend

$A \geq 1.62 \times 10^{-3}$ m. It would be expected that ω_0 be independent of the amplitude but, interestingly, the value for A where the change of behavior is observed coincides with that of the inset in Fig. 4b. We attribute this behavior to two possible reasons. On the one hand, this feature could be associated with a viscosity effect in the bridge. It should be noted again that the relative viscous/capillary effect for the case of smaller amplitudes is more important than for higher amplitudes (Fig. 8), affecting the liquid bridge response in a noticeably way in the first case. On the other hand, the theoretical prediction by Eq. (7) (Fig. 10) is less accurate for lower amplitudes.

Considering the vast knowledge regarding the modeling of dry granular systems when static or quasi-static conditions apply, the description of the forces acting among particles is very well accomplished through elastic contact-force models plus viscosity terms. When humidity is also present in this scenario, the addition of a capillary term is necessary, but the contact forces remain the same. Even more, if the relative movement among particles is performed at low velocities, the liquid viscosity term can be neglected. Nevertheless, for the case of wet granular systems subjected to considerably movement, contact elastic forces may be absent much of the time and capillary and liquid viscous effects dominate. The results presented here demonstrate that an "anti" elastic capillary force (Eq. (2)) is able to describe the dynamics of the vibration of a particle, even neglecting viscous effects, given a solution quite different to that for an elastic bridge deformation. The consideration of the forces intervening in the dynamics given by Eq. (5) is appropriate as soon as the deformation of the bridge be high enough (order of 1.62×10^{-3} and higher) and the rate of deformation be sufficiently low ($C_a < 10^{-1}$).

Although evidence of the role of viscosity is appreciated from the present experiments, we can state that viscosity effects can be neglected when modeling the oscillations of a sphere-liquid bridge system at appreciable amplitudes.

6 Conclusion

This work analyzed the dynamical behavior of a capillary bridge between a spherical particle and a plane surface subjected to a vertical oscillatory motion. The influence of the amplitude and the oscillation frequency of the plane, as well as the volume of the capillary bridge at the moment of capillary bridge rupture, were analyzed to set up the proper conditions for the experiments.

The rate of increase of the frequency was found to have little influence on the breakage of the capillary bridge, or its geometry just prior to breakage.

As expected, the volume of the capillary bridge influenced not only the static capillary force but also the dynamical behavior of the bridge, giving a higher frequency for rupture as the liquid volume increased.

The amplitude of the oscillations, A, also played an important role. Although the geometrical parameters of the bridge before breaking shown to be independent of A, we found an inverse dependence between the frequency for rupture and the amplitude.

The oscillation of the sphere/liquid-bridge system was systematically studied as a function of the amplitude and at a fixed frequency. From the set of data obtained, we were able to determine the deformation of the bridge and the dynamics of the sphere attached to it.

Two different regimes were found for the correlation between the maximum deformation of the bridge and the amplitude of the oscillations. For smaller A, the bridge resulted to be more resistant to deformation than for larger ones. This behavior was found consistent with the evaluation of the capillary and viscous forces involved in the problem, which demonstrated that viscous effects were important for $A \geq 1.62 \times 10^{-3}$. For this range of amplitudes, it was observed that viscosity effects are only important during the first milliseconds of the bridge stretching and the last milliseconds of the bridge contraction.

By neglecting the viscous effects and assuming that the angles involved in the bridge geometry were constant along the deformation period, a tractable differential equation could be derived and solved. This equation was able to correctly describe the experimental behavior at all amplitudes with only one free fitting parameter.

The analysis of the values attained by the parameters of the equation (ω_0, F_0, G_0) related to the single free fitting parameter when the amplitude varied showed two important aspects. In first place, F_0 (and so G_0), increased as A increased. This represented the effect of the weakening of the liquid bridge for greater amplitudes, allowing a further deformation of the bridge and, consequently, a smaller average value of the angle β formed between the center of the sphere and the inception of the liquid bridge. Secondly, it was observed that ω_0 (capable of being interpreted as a characteristic frequency of the system) reached a constant value when $A \geq 1.62 \times 10^{-3}$ m, when the viscous effects are expected to be negligible.

The theoretical description here proposed has demonstrated to be useful to represent the dynamics of a liquid bridge for a particle subjected to an oscillatory movement as soon as the amplitude of those oscillations are greater enough to avoid viscous effects. This conclusion has important consequences when modelling the manipulation of granular matter under the presence of humidity, i.e., when important relative displacements between grains are expected and the static capillary models could be questionable.

Future efforts will be conducted to study in detail the behavior of the geometry of the bridge, represented here by β, as a function of the deformation in a first stage and, secondly, to change the viscous properties of the liquid in order to quantify even better the role of viscous forces during the bridge deformation run.

Acknowledgements This work has been done with financial support from Universidad Nacional de San Luis under the Project PROICO 03-2718 and the International Foundation Program of the University of Navarra. AFV wishes to thank the hospitality received by the Department of Physics and Applied Mathematics during her working stay at the Group of Granular Media, where part of the experiments was developed.

Funding Funding was provided by Universidad Nacional de San Luis (Grant No. 032718) and Consejo Nacional de Investigaciones Científicas y Técnicas (Grant No. PIP 11220170100245) and International Foundation Program of the University of Navarra.

Declarations

Conflict of interest The authors declare that they have no conflict of interest regarding the publication of this article.

References

1. O'Hern, C.S.: Computational methods. In: Franklin, S.V., Shattuck, M.D. (eds.) Handbook of Granular Materials, pp. 119–154. CRC Press, Taylor & Francis, Cambridge (2016)
2. Duran, J.: Sands, Powders, and Grains: An Introduction to the Physics of Granular Materials. Springer, New York (2000)
3. Blair, D.L., Kudrolli, A.: Magnetized granular materials. In: Hinrichsen, H., Wolf, D.E. (eds.) The Physics of Granular Media, pp. 281–296. Wiley, Weinheim (2004)
4. Cundall, P.A., Strack, O.D.L.: A discrete numerical model for granular assemblies. Géotechnique **29**, 47–65 (1979)
5. Savage, S.B.: Disorder, diffusion, and structure formation in granular flows. In: Bideau, D. (ed.) Disorder and Granular Media, pp. 255–287. North Holland, Amsterdam (1993)
6. Herminghaus, S.: Dynamics of wet granular matter. Adv. Phys. **54**, 221–244 (2005)
7. Crassous, J., Ciccotti, M., Charlaix, E.: Capillary force between wetted nanometric contacts and its application to atomic force microscopy. Langmuir **27**, 3468–3473 (2011)
8. Mitarai, N., Nori, F.: Wet granular materials. Adv. Phys. **55**, 1–45 (2006)
9. Abdullah, M., Rahmayanti, H.D., Amalia, N., Yuliza, E., Munir, R.: Effective elastic modulus of wet granular materials derived from modified effective medium approximation and proposal of an equation for the friction coefficient between the object and wet granular materials surfaces. Granul. Matter **23**, 78 (2021)
10. Moharamkhani, H., Sepehrinia, R., Taheri, M., Jalalvand, M., Brinkmann, M., Vaez-Allaei, S.M.: Ordered/disordered monodisperse dense granular flow down an inclined plane: dry versus wet media in the capillary bridge regime. Granular Matter 23, 62, and references there in. (2021)
11. Anand, A., Curtis, J.S., Wassgren, C.R., Hancock, B.C., Ketterhagen, W.R.: Predicting discharge dynamics of wet cohesive particles from a rectangular hopper using the discrete element method (DEM). Chem. Eng. Sci. **64**, 5268–5275 (2009)

12. Lievano, D., Velankar, S., McCarthy, J.J.: The rupture force of liquid bridges in two and three particle systems. Powder Technol. **313**, 18–26 (2017)
13. Ziskind, G., Fichman, M., Gutfinger, C.: Particle behavior on surfaces subjected to external excitations. J. Aerosol. Sci. **31**, 703–719 (2000)
14. Valenzuela Aracena, K.A., Benito, J.G., Oger, L., Ippolito, I., Uñac, R.O., Vidales, A.M.: Frequency-amplitude behavior for incipient movement of grains under vibration. Particuology **40**, 1–9 (2018)
15. Perales, J.M., Meseguer, J.: Theoretical and experimental study of the vibration of axisymmetric viscous liquid bridges. Phys. Fluids **4**, 1110–1130, and references there in (1992)
16. Valsamis, J.-B., Mastrangeli, M., Lambert, P.: Vertical excitation of axisymmetric liquid bridges. Eur. J. Mech. B. Fluids **38**, 47–57 (2013)
17. Ichikawa, N., Kawaji, M., Misawa, M., Psofogiannakis, G.: Resonance behavior of a liquid bridge caused by horizontal vibrations. J. Jpn. Soc. Microgravity Appl. **20**, 292–300 (2003)
18. Liang, R.-Q., Kawaji, M.: Surface oscillation and flow structure of a liquid bridge under small vibration. Chin. Phys. Lett. **31**, 044701 (2014)
19. Benilov, E.S.: Stability of a liquid bridge under vibration. Phys. Rev. E **93**, 063118 (2016)
20. Haynes, M., Vega, E.J., Herrada, M.A., Benilov, E.S., Montanero, J.M.: Stabilization of axisymmetric liquid bridges through vibration-induced pressure fields. J. Colloids Interface Sci. **513**, 409–417 (2018)
21. Pitois, O., Moucheront, P., Chateau, X.: Liquid bridge between two moving spheres: an experimental study of viscosity effects. J. Colloid Interface Sci. **231**, 26–31 (2000)
22. Bozkurt, M.G., Fratta, D., Likos, W.J.: Capillary forces between equally sized moving glass beads: an experimental study. Can. Geotech. J. **54**, 1300–1309 (2017)
23. Agarwal, P., Murdande, R.M., Kandaswamy, A.S., Bobji, M.S.: Dynamic stretching of a liquid bridge. Int. J. Adv. Eng. Sci. Appl. Math. **11**, 238–243 (2019)
24. Ennis, B.J., Li, J., Tardos, G.I., Pfeffer, R. (1990) The influence of viscosity on the strength of an axially strained pendular liquid bridge. Chem. Eng. Sci. **45**, 3071–3088
25. Maugis, D.: Adherence of elastomers: fracture mechanics. J. Adhes. Sci. Technol. **1**, 105–134 (1987)
26. Sudo, S., Innami, S., Matsumoto, K.: Vibration characteristics of liquid bridge between sphere and a solid base subject to vertical vibration. J. JSEM **12**, s51–s56 (2012)
27. Buck, B., Lunewski, J., Tang, Y., Deen, N.G., Kuipers, J.A.M., Heinrich, S.: Numerical investigation of collision dynamics of wet particles via force balance. Chem. Eng. Res. Des. **132**, 1143–1159 (2018)
28. Pu, C., Liu, F., Wang, S.: Liquid force and rupture distance between two particles. Adv. Mater. Sci. Eng., Article ID3542686 (2021)
29. Butt, H.-J., Kappl, M.: Normal capillary forces. Adv. Colloids Interface Sci. **146**, 48–60 (2009)
30. Matthewson, M.J.: Adhesion of spheres by thin liquid films. Philos. Mag. A **57**, 207–216 (1988)